EPJ Web of Conferences **17**, 10004 (2011)
DOI: 10.1051/epjconf/20111710004

Production of doubly magic nucleus ^{100}Sn in ^{72,74,76}Kr+^{40}Ca, ^{72,74,76}Kr+^{40}Ar and ^{72,74,76}Kr+^{32}S reactions at $4-6$ MeV/nucleon

Sh.A. Kalandarov[1,a], G.G. Adamian[1], N.V. Antonenko[1], and J.P. Wieleczko[2]

[1] Joint Institute for Nuclear Research, 141980 Dubna, Russia
[2] GANIL, CEA et IN2P3-CNRS, B.P. 55027, F-14076, Caen Cedex, France

Abstract. The mechanism of production of evaporation residues in low energy fusion reactions is investigated within the dinuclear system model. The model predictions for the production cross sections of exotic nuclei are compared with the available experimental data. The possibilities of production of doubly magic nucleus ^{100}Sn via particle evaporation channels and ^{12}C emission channel in the reactions ^{72,74,76}Kr+^{40}Ca, ^{72,74,76}Kr+^{40}Ar and ^{72,74,76}Kr+^{32}S are investigated at bombarding energies $4-6$ MeV/nucleon.

1 Introduction

The reactions with radioactive ions are of great interest for experimental and theoretical studies. The experiments with neutron-rich and neutron-deficient nuclei open a new doors for the investigation of the properties of nuclear matter under extreme N/Z-ratio and can lead to production of still unknown isotopes.

There were several experimental attempts to produce doubly magic nucleus ^{100}Sn which is very difficult to reach. The first mass measurement of ^{100}Sn was performed in GANIL, where it was produced with the fusion-evaporation reaction ^{50}Cr + ^{58}Ni at energy of 5.1 MeV/nucleon [1]. The reported production cross section for ^{100}Sn was 40 nb. Production of very neutron-deficient isotopes near doubly magic ^{100}Sn nucleus via light particle evaporation channels and cluster emission channel was considered in Ref. [2] in the ^{58}Ni + ^{50}Cr and ^{58}Ni + ^{58}Ni reactions. Authors of this work concluded that both types of reactions yield similar cross sections for the production of exotic nuclei near ^{100}Sn. Another possibility of producing ^{100}Sn is reported in Ref. [3] via the ^{54}Fe(^{58}Ni,4n) ^{108}Xe reaction that allows us to reach ^{100}Sn with the ^{108}Xe–^{104}Te–^{100}Sn alpha decay chain.

Here, we suggest one more possibility for producing exotic nuclei around ^{100}Sn by using the reactions ^{72,74,76}Kr + ^{40}Ca, ^{72,74,76}Kr+ ^{40}Ar and ^{72,74,76}Kr+^{32}S at $4-6$ MeV/nucleon. The main idea is to create the excited compound nucleus (CN) with $Z = 50 + 2, 4, 6$ in fusion reactions and look for the evaporation channels with light particles and heavier clusters like ^{12}C which will finally lead to the evaporation residue near doubly magic nucleus ^{100}Sn. Since the proton emission channel becomes stronger in such an excited neutron-deficient CN, the suggested ^{72,74,76}Kr+^{40}Ca reactions can lead to better conditions for the formation of ^{108}Xe and further use of alpha decay chain ^{108}Xe–^{104}Te–^{100}Sn. The calculations of the cross sections are performed within the dinuclear system (DNS) model, which was successfully applied to the description of charge and mass distributions of decay products in low energy nuclear reactions [4,5]. The DNS model has been successful in describing the isospin dependence measured for the ^{78,82}Kr + ^{40}Ca fusion reactions at GANIL with INDRA [6] and confirmed by the recent ISODEC experiment at Catania with CHIMERA [7].

[a] e-mail: shuhrat@theor.jinr.ru

2 Model

The DNS model [4,8] describes an evolution of the charge and mass asymmetry degrees of freedom, which are defined here by the charge and mass (neutron) numbers $Z = Z_1$ and $A = A_1$ ($N = N_1 = A - Z$) of light nucleus of the DNS formed in the entrance channel of the reaction after the dissipation of the kinetic energy and angular momentum of relative motion. According to this description, there are nucleon drift and nucleon diffusion between the DNS nuclei and eventually either a CN is formed (the complete fusion) or the DNS with given Z and A is formed and decays (quasifission). After the formation, the excited CN decays by various channels including the formation of certain DNS and their decay. The competition between the complete fusion and quasifission processes depends on the value of maximum angular momentum deposited in the system. The quasifission and CN decays are hardly distinguished in the experiments because in both cases two fragments are produced with and without stage of the CN formation.

The cross section of the binary decay is calculated as follows [4]

$$\sigma_{Z,A}(E_{\mathrm{c.m.}}) = \sum_{J=0}^{J_{max}} \sigma_{cap}(E_{\mathrm{c.m.}}, J) W_{Z,A}(E^*_{CN}, J), \qquad (1)$$

where σ_{cap} is the partial capture cross section which defines the transition of the colliding nuclei over the Coulomb barrier and the formation of the initial DNS when the kinetic energy and angular momentum J of the relative motion are transformed into the excitation energy and angular momentum of the DNS. The transition probability is calculated with the Hill-Wheeler formula. The value of $W_{Z,A}(E^*_{CN}, J)$ is the formation-decay probability of the DNS with a given asymmetries Z and A. The probability of the DNS formation is statistically calculated by using the stationary solution of the master equation with respect to the charge and mass asymmetries and depends on the potential energy of the DNS configurations and on the thermodynamical temperature. The probability of the DNS decay in R coordinate is calculated by using the transition state method. This probability depends on the difference between the potential energies of the DNS configurations at the touching distance and at the barrier position. The maximum value of angular momentum J_{max} is limited by either the kinematical angular momentum $J_{kin} = [2\mu(E_{\rm c.m.} - V(R_b))/\hbar^2]^{1/2}R_b$ (R_b is the position of the Coulomb barrier with the height $V(R_b)$ and μ is the reduced mass) or by the critical angular momentum J_{cr} depending on which one is smaller: $J_{max} = \min[J_{kin}, J_{cr}]$. The details of calculations of σ_{cap}, $W_{Z,A}(E^*_{CN}, J)$, and, correspondingly, $\sigma_{Z,A}(E_{\rm c.m.})$ are given in Ref. [4]. Here, only the most salient features are outlined.

The DNS model describes the evolution of interacting nuclei along two degrees of freedom: the relative distance R between the center of the nuclei, the charge and mass-asymmetry degrees of freedom, which are defined here by the charge Z and mass A of the light partner of the DNS. After the dissipation of kinetic energy and angular momentum of the relative motion, the DNS is trapped in the pocket of the interaction potential between partners. Then, a statistical equilibrium is reached in the mass-asymmetry coordinate so that the formation probability $P_{Z,A}$ of each DNS or CN configuration depends on the potential energy $U(R_m, Z, A, J)$, calculated with respect to the potential energy of the rotational CN where R_m is the location of the minimum of the pocket in the nucleus-nucleus interaction potential. After the capture stage, there are nucleon drift and nucleon diffusion between the nuclei which constitute the DNS. Then, the excited DNS can decay with a probability $P^R_{Z,A}$ in R if the local excitation energy of the DNS is high enough to overcome the barrier in the nucleus-nucleus potential. Ultimately, the system evolves either towards a CN configuration that subsequently decays, or to a DNS configuration. The latter process, in which a two-body configuration is kept along the trajectory, is the quasifission phenomenon.

The emission probability $W_{Z,A}(E^*_{CN}, J)$ of a fragment (Z,A) is calculated as the product of the DNS formation probability and the DNS decay probability:

$$W_{Z,A}(E^*_{CN}, J) = \frac{P_{Z,A}P^R_{Z,A}}{\sum_{Z',A'} P_{Z',A'}P^R_{Z',A'}}, \qquad (2)$$

where the indexes Z' and A' goes over all possible channels from the neutron evaporation to the symmetric splitting. The probability $P_{Z,A}$ is the equilibrium limit of the master equation (see [4] for details) given by

$$P_{Z,A}(E^*_{CN}, J) \sim \exp[-U(R_m, Z, A, J)/T_{CN}(J)]. \qquad (3)$$

Here, the n, p, d and t-evaporation channels are taken into consideration with $U(R_m, Z, A, J)$=0. The quasifission barrier B^{qf}_R, calculated as the difference between the bottom of the inner pocket and the top of the external barrier, prevents the decay of the DNS along the R-degree of freedom with the weight $P^R_{Z,A}$ given as

$$P^R_{Z,A} \sim \exp[-B^{qf}_R(Z, A, J)/T_{Z,A}(J)]. \qquad (4)$$

In Eqs. (3) and (4) $T_{CN}(J)$ and $T_{Z,A}(J)$ are the temperatures of the CN and the DNS, respectively. For the emission of particles with $Z < 2$, $T_{Z,A}(J) = T_{CN}(J)$ and $B^{qf}_R(Z, A, J)$ is equal to the particle binding energy plus the value of the Coulomb barrier at $Z \neq 0$. The Fermi-gas model is employed to compute the temperature, with a level-density parameter $a = 0.114A + 0.162A^{2/3}$.

In the calculations, we use the formulas (1) and (2) to treat the sequential statistical decay (the evaporation of light particles and/or the binary decay) of the hot CN. The generation of whole cascade of decay channels is performed by the Monte Carlo method. We continue to trace the decay processes until all fragments become cold (the excitation energy of fragments is smaller than its neutron emission threshold). The number n of generation of the events in the Monte Carlo technique was chosen according to the smallest decay probability which is $\sim 1/n$.

3 Results and discussion

Since DNS model is able to reproduce charge and mass distributions of complex fragments produced in fusion and quasifission reactions[4–6], we check also the ability of the model to reproduce light charged particle multiplicities in the different reactions. We calculate the total multiplicities of protons and alpha particles and made comparisons with the experimental data from Refs. [10–13]. We have found the agreement between our calculations and experimental data for total proton and alpha particle multiplicities within 20 − 30%. Thus, our model can give reasonable estimates of ER's production cross sections via light particle evaporation channels and cluster emission channels.

In Table 1, we present the comparison of our model predictions with available experimental data on production cross sections of residues near ^{100}Sn. Overall agreement is rather good, though in some cases our model overestimates the experimental data by 6 − 8 times. The competition between the formation channels depends on available excitation energy and angular momentum. For the ^{58}Ni+^{58}Ni reaction, with increasing excitation energy the ^{12}C emission channel gives smaller contribution to the formation of residual nuclei ^{100}In and ^{101}Sn because after the emission of ^{12}C more excitation energy is left in the system and further emission of charged particles results in residual nucleus with lower Z. Thus, this channel becomes possible

Table 1. Comparison of calculated production cross sections with the experimental data. The weights of main formation channels are derived from our calculations. Experimental values are taken from Refs. [1–3]

reaction	E_{lab}(MeV)	E^*_{CN}(MeV) at J=0	J_{max}	ER	$\sigma_{Exp.}$(mb)	$\sigma_{cal.}$(mb)	formation channel
^{58}Ni+^{50}Cr	319	102	75	^{100}In	2.6×10^{-3}	8.3×10^{-3}	$\alpha p3n$
^{58}Ni+^{58}Ni	325	96	78	^{100}In	0.8×10^{-3}	2.8×10^{-3}	$^{12}Cp3n$(80%),$3\alpha p3n$(20%)
^{58}Ni+^{58}Ni	348	107	78	^{100}In	1.7×10^{-3}	7.7×10^{-3}	$^{12}Cp3n$(60%),$3\alpha p3n$(40%)
^{58}Ni+^{58}Ni	371	119	78	^{100}In	1.7×10^{-3}	4.6×10^{-3}	$^{12}Cp3n$(40%),$3\alpha p3n$(60%)
^{58}Ni+^{58}Ni	394	131	78	^{100}In	1.6×10^{-3}	6.1×10^{-4}	$^{12}Cp3n$(10%),$3\alpha p3n$(90%)
^{58}Ni+^{50}Cr	249	70	64	^{101}Sn	$(1.6\pm0.4)\times10^{-5}$	7.4×10^{-5}	$\alpha 3n$
^{58}Ni+^{58}Ni	325	96	78	^{101}Sn	$(0.9\pm0.4)\times10^{-5}$	4.4×10^{-5}	$^{12}C3n$(70%), $3\alpha3n$(30%)
^{58}Ni+^{58}Ni	348	107	78	^{101}Sn	$(1.3\pm0.3)\times10^{-5}$	6.2×10^{-5}	$^{12}C3n$(50%), $3\alpha3n$(50%)
^{58}Ni+^{58}Ni	371	119	78	^{101}Sn	$(2.8\pm1.0)\times10^{-5}$	5.4×10^{-5}	$^{12}C3n$(35%), $3\alpha3n$(65%)
^{58}Ni+^{58}Ni	394	131	78	^{101}Sn	$(0.7\pm0.4)\times10^{-5}$	0.4×10^{-5}	$^{12}C3n$(5%), $3\alpha3n$(95%)
^{58}Ni+^{54}Fe	200	40	27	^{110}Xe	$(1.0\pm0.2)\times10^{-3}$	4.4×10^{-4}	$2n$
^{58}Ni+^{54}Fe	215	47	40	^{109}Xe	$(1.0\pm0.2)\times10^{-5}$	5.4×10^{-5}	$3n$
^{50}Cr+^{58}Ni	255	92	75	^{100}In	1.0×10^{-3}	5.2×10^{-4}	$\alpha p3n$
^{50}Cr+^{58}Ni	255	92	75	^{100}Sn	4.0×10^{-5}	2.4×10^{-6}	$\alpha 4n$

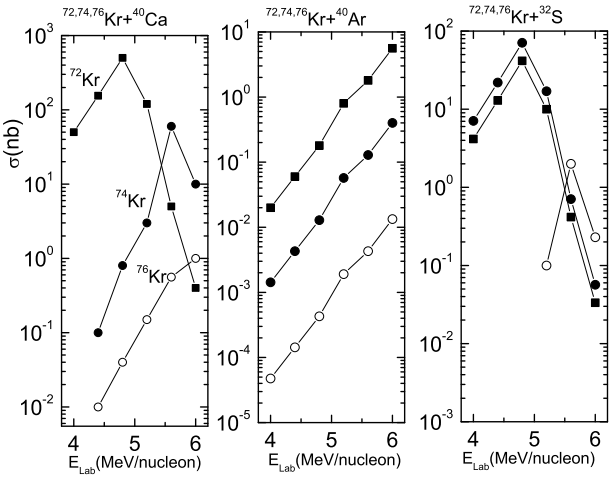

Fig. 1. Excitation functions for the production of ^{100}Sn in the reactions ^{72,74,76}Kr+^{40}Ca, ^{72,74,76}Kr+^{40}Ar and ^{72,74,76}Kr+^{32}S at 4 – 6 MeV/nucleon. Open circles are for ^{76}Kr, solid circles are for ^{74}Kr, and solid squares are for ^{72}Kr.

only at high angular momentums where less excitation energy is available and also higher probability for emission of ^{12}C. But at angular momentums $J > 60$, the quasifission process from nearly symmetric configurations dominates and the evaporation residue cross section strongly decreases. 3α channel takes away almost twice more excitation energy than the ^{12}C emission channel. Therefore, at high excitation energies the main formation channel of residual nuclei ^{100}In and ^{101}Sn is related to the 3α channel. Since the CN formed in these reactions are neutron-deficient, the multiple neutron emission is strongly suppressed. Authors of Ref. [3] have proposed an alternative method to create residual nucleus ^{100}Sn. They suggested to use $4n$ decay channel in the reaction ^{58}Ni+^{54}Fe which yields the residual nucleus ^{108}Xe and further alpha decay chain results in the residual nucleus ^{100}Sn. Our calculations indicate that the $4n$ decay channel has a cross section of $\sim$ 0.1 nb at $E_{lab} = 240$ MeV. If one uses ^{56}Ni+^{58}Ni reaction with $\alpha 2n$ decay channel, then at $E_{lab} = 270$ MeV one can obtain the residual nucleus ^{108}Xe with the cross section of $\sim$ 30 nb.

We calculate the formation cross sections for the residual nucleus ^{100}Sn in the reactions ^{72,74,76}Kr + ^{40}Ca, ^{72,74,76}Kr + ^{40}Ar, and ^{72,74,76}Kr+^{32}S at 4 – 6 MeV/nucleon, which form the compound nuclei with $Z = 50 + 2, 4, 6$. The excitation functions for the production of ^{100}Sn in these reactions are given in Fig. 1. The cross sections for formation of residual nucleus ^{100}Sn are largest for the ^{72}Kr+^{40}Ca reaction, in which ^{12}C and 3α decay channels play a role. At low energies, only ^{12}C decay channel can form the residual nucleus ^{100}Sn, while the 3α channel requires more energy. At higher energies, the 3α decay channel starts to dominate in the formation of ^{100}Sn because only this channel can take away all excitation energy. With increasing excitation energy of CN at $J = 0$ ^{100}Sn can be formed only at high angular momentums due to the decrease of available excitation energy with J. Predicted cross section for the production of ^{100}Sn has the maximum value 500 nb at 4.8 MeV/nucleon bombarding energy. This value is more than one order of magnitude larger than one achieved so far. With increasing N/Z–ratio in the system the cross sections drop strongly down due to the larger role of neutron emission and higher emission barriers for charged particles. Besides the direct production of ^{100}Sn via the decay channels, one can look for the production of residual nuclei ^{108}Xe and ^{104}Te. In the ^{72}Kr+^{32}S reaction one can form the CN ^{104}Te, but unfortunately, this compound nucleus is excited and decays via different decay channels. One can use the ^{74}Kr+^{32}S reaction and the $2n$ decay channel to produce ^{104}Te, but at lower bombarding energies than considered here. ^{108}Xe can be formed with the cross section $\sim$ 10 nb in the ^{72}Kr+^{40}Ca reaction via the decay channel $2p2n$ or in the ^{74}Kr+^{40}Ca reaction via the $\alpha 2n$ decay channel. As follows from our calculations, these decay channels have more than one order of magnitude higher cross sections than the $4n$ channel which was suggested in Ref. [3] for the reaction ^{58}Ni+^{54}Fe.

Table 2. Calculated weights of formation channels and production cross sections for ^{100}Sn.

reaction	E_{lab}(MeV/nucleon)	E^*_{CN}(MeV) at J=0	J_{max}	$\sigma_{cal.}$(nb)	formation channel
^{72}Kr+^{40}Ca	4.0	48	38	50	^{12}C
^{72}Kr+^{40}Ca	4.4	58	52	155	^{12}C(80%),3α(20%)
^{72}Kr+^{40}Ca	4.8	68	63	500	^{12}C(60%),3α(40%)
^{72}Kr+^{40}Ca	5.2	79	68	120	^{12}C(10%),3α(90%)
^{72}Kr+^{40}Ca	5.6	89	68	5	3α
^{72}Kr+^{40}Ca	6.0	99	68	0.4	3α
^{74}Kr+^{40}Ca	4.4	62	54	0.1	$^{12}C2n$
^{74}Kr+^{40}Ca	4.8	72	65	0.8	$^{12}C2n$
^{74}Kr+^{40}Ca	5.2	83	69	3	$^{12}C2n$(80%),3$\alpha 2n$(20%)
^{74}Kr+^{40}Ca	5.6	93	69	60	$^{12}C2n$(50%),3$\alpha 2n$(50%)
^{74}Kr+^{40}Ca	6.0	103	69	10	$^{12}C2n$(40%),3$\alpha 2n$(60%)
^{72}Kr+^{32}S	4.0	55	37	4.16	$2p2n$
^{72}Kr+^{32}S	4.4	64	49	12.9	$2p2n$
^{72}Kr+^{32}S	4.8	73	56	41.6	$2p2n$
^{72}Kr+^{32}S	5.2	82	63	10	$2p2n$
^{72}Kr+^{32}S	5.6	91	63	0.41	$2p2n$
^{72}Kr+^{32}S	6.0	100	63	0.033	$2p2n$
^{74}Kr+^{32}S	4.0	59	39	7	$\alpha 2n$
^{74}Kr+^{32}S	4.4	69	51	22	$\alpha 2n$
^{74}Kr+^{32}S	4.8	78	58	71	$\alpha 2n$
^{74}Kr+^{32}S	5.2	86	65	17	$\alpha 2n$
^{74}Kr+^{32}S	5.6	97	65	0.7	$\alpha 2n$
^{74}Kr+^{32}S	6.0	104	65	0.057	$\alpha 2n$(90%) $2p4n$(10%)

4 Conclusion

Production of exotic nuclei around ^{100}Sn in the fusion reactions was theoretically investigated within the DNS model. Comparisons of calculated results with the available experimental data shows the satisfactory agreement. Within such an accuracy the production rates for ^{100}Sn in fusion reactions^{72,74,76}Kr+^{40}Ca, ^{72,74,76}Kr+^{40}Ar, and ^{72,74,76}Kr+^{32}S were calculated at bombarding energy of 4−6 MeV/nucleon with the 0.4 MeV/nucleon energy step. As shown, the maximal yield for ^{100}Sn corresponds to the reaction ^{72}Kr+^{40}Ca at 4.8 MeV/nucleon, which is as high as 500 nb. In order to use super-allowed alpha-decay chain ^{108}Xe–^{104}Te–^{100}Sn to produce the nucleus ^{100}Sn, the reactions ^{72}Kr+^{40}Ca and ^{74}Kr+^{40}Ca were suggested to produce ^{108}Xe with the cross section ∼ 10 nb via the $2p2n$ and $\alpha 2n$ decay channels. At lower energies than considered here, one can use the ^{74}Kr+^{32}S reaction to produce ^{104}Te via the $2n$ channel. It is also possible to produce the residual nucleus ^{108}Xe in the ^{56}Ni+^{58}Ni reaction via the $\alpha 2n$ decay channel at E_{lab} = 270 MeV with the cross section of ∼ 30 nb.

This work was supported by DFG and RFBR. IN2P3 - JINR and Polish-JINR Cooperation programs are gratefully acknowledged.

References

1. M. Chartier *et al.*, Phys. Rev. Lett. **77**, 2400 (1996).
2. M. La Commara *et al.*, Nucl. Phys. **A669**, 43 (2000).
3. A. Korgul *et al.*, Phys. Rev. C **77**, 034301(2008).
4. Sh.A. Kalandarov, G.G. Adamian, N.V. Antonenko and W. Scheid, Phys. Rev. C **82**, 044603 (2010).
5. Sh.A. Kalandarov *et al.*, Phys. Rev. C **83**, 054611 (2011).
6. G. Ademard *et al.*, Phys. Rev. C **83**, 054619 (2011); G. Ademard *et al.*, Proc. Int. Conf. Fusion11, Saint-Malo, France (2011), in print.
7. S. Pirrone *et al.*, Proc. Int. Conf. Fusion11, Saint-Malo, France (2011), in print.
8. V.V. Volkov, Izv. AN SSSR ser. fiz. **50**, 1879 (1986); G.G. Adamian, A.K. Nasirov, N.V. Antonenko, and R.V. Jolos, Phys. Part. Nucl. **25**, 583(1994); G.G. Adamian, N.V. Antonenko, and W. Scheid, Nucl. Phys. **A618**, 176 (1997); G.G. Adamian, N.V. Antonenko, W. Scheid, and V.V. Volkov, Nucl. Phys. **A627**, 361 (1997); G.G. Adamian, N.V. Antonenko, W. Scheid, and V.V. Volkov, Nucl. Phys. **A633**, 409 (1998); G.G. Adamian, N.V. Antonenko, and W. Scheid, Phys. Rev. C **68**, 034601 (2003).
9. G.G. Adamian, N.V. Antonenko, W. Scheid, Lecture Notes in Physics, Clusters in Nuclei, Vol. **2**, ed. by C. Beck (Springer, Berlin, 2011), in print.
10. E. Vardaci *et al.*, Eur. Phys. J. **A43**, 127 (2010).
11. J. Galin *et al.*, Phys. Rev. C **9**, 1113 (1974).
12. J. Boger *et al.*, Phys. Rev. C **49**, 1576 (1994).
13. M. Gonin *et al.*, Phys. Rev. C **42**, 2125 (1990).